

Research Paper

Numerical Solution of MHD Casson Fluid Flow Due to a Moving Extensible Surface with Second-Order Velocity Slip and Carbon Nanotubes

Reddissekhar Reddy SEETHI REDDY, Bala Anki Reddy POLU

Department of Mathematics
S.A.S., VIT University
Vellore-632014, India

e-mail: reddyshekara43@gmail.com, pbarmaths@gmail.com

This theoretical research work deals with the effect of aligned magnetic field flow and heat transfer of carbon nanotubes towards a nonlinear stretching sheet. In addition, we have considered two kinds of carbon nanotubes, namely SWCNTs and MWCNTs, used with water as the base fluid. The governing boundary layer flow equations narrating partial differential equations are transformed into a system of ordinary differential equations with the assistance of similarity transformation. Obtained coupled non-linear differential equations are solved by fourth-order Runge-Kutta (R-K) method along with shooting technique. A comparative study of the formerly published results and the present results for a special case shows that all these results are in an excellent agreement.

Key words: aligned magnetic field; thermal radiation; carbon nanotubes; slip model and Casson fluid.

1. INTRODUCTION

Recently, the research work concerning flow over a stretching sheet has produced great interest due to its abundant industrialized applications. For example, in the preservation of bath, the boundary layer along physical management conveyers, the production of canvas materials over an expulsion procedure, the sweptback extrusion of soft sheer crystal and ported over a moving incessant solid surface in a critical kind of flow arising in various engineering processes. Thermal radiation effects on the flow over a stretching sheet, in the existence of the transverse magnetic field, were examined by REDDY and REDDY [1]. SRINIVAS *et al.* [2] presented the effects of a chemical reaction on an unsteady flow of a micropolar fluid in the direction of a permeable stretching sheet embedded

in a non-Darcian porous medium. The stagnation nano-energy conversion problems were studied for conjugate mixed convection heat and mass transfer with EMHD (electrical magnetohydrodynamic) field over a slip boundary stretching surface by HSIAO [3]. AHMED *et al.* [4] examined the magnetohydrodynamic axisymmetric flow of power-law fluid model of an unsteady radially stretching sheet under the influence of convective boundary conditions. A new numerical method for solving the stagnation-point flow problem over a permeable stretching/shrinking sheet in porous media was employed by BHATTI *et al.* [5]. Different types of fluid models subject to a stretching sheet have been reported by many researchers [6–11]. Recently, KHAN *et al.* [12] have analyzed the thermal and concentration diffusion in Jeffery nanofluid flow over an inclined stretching surface. The computational solution of the problem addressing the variable viscosity and inclined Lorentz force effects on Williamson nanofluid over a nonlinear stretching sheet was explored by KHAN *et al.* [13]. Flows due to a moving extensible surfaces were examined by some authors [14–16].

Non-Newtonian fluid flow problems in fluid mechanics draw great attention because of their unique challenge for engineers, physicists, and mathematicians. The Casson fluid model is one of the non-Newtonian fluid models depends on the intuitive conduct of solid phase suspension and liquid phase suspension. In this model, yield stress is dominant as compared to shear stress. In addition, a material having features of Casson fluid may reflect solid characteristics when shear stress is significantly smaller in contrast to yield stress. The examples of the Casson fluids are human blood, jelly, honey, soup and concentrated fruit juices. MUKHOPADHYAY [17] demonstrated the non-Newtonian fluid flow over a nonlinearly stretching surface. RAMESH and DEVIKAR [18] studied three fundamental flows of an incompressible Casson fluid between parallel plates. They found the analytical solutions of Couette, generalized Couette and Poiseuille flows under slip boundary conditions. The effects of MHD on the blood flow, when blood is represented as a non-Newtonian fluid, over a horizontal cylinder were studied by FARHAD ALI *et al.* [19]. SUBBA RAO ANNASAGARAM *et al.* [20] examined the boundary layer flow of a hydromagnetic, non-Newtonian nanofluid flow over a vertical cone with partial slip. Lie group transformation on magnetohydrodynamic double-diffusion convection of a non-Newtonian nanofluid over a vertical stretching or shrinking surface was made by PAL and ROY [21]. Afterward, various studies were made on Casson fluid by different researchers by considering distinct physical effects; one can assess the concerned literature in [22–27]. The first-order, 1.5-order and second-order slip models [28] have not yet been discussed elaborately in the existing literature. Moreover, these models are considered with the progress of micro/nano technologies, as the measurement capacities of micro/nanoscale gadgets are every now and again stretched to the furthest reaches of altogether smaller than the mean free way of gas particles, i.e.,

high Knudsen number gas flows. Regular cases are gas flows inside nanotubes, and air oil of head-plate interface of circle drives to say only a couple.

To the author’s knowledge, no studies have been reported on effects of Casson fluid flow and aligned magnetic field on steady two-dimensional flow over a moving extensible surface with velocity slip and carbon nanotubes. The main objective of the present paper is to analyze the influences of an aligned magnetic field on the boundary layer flow of a Casson fluid over a stretching sheet in the presence of carbon nanotubes with velocity slip effect. The governing non-linear momentum and thermal boundary layer equations are transformed into a system of ordinary differential equations using similarity transformation. The obtained coupled non-linear differential equations are solved by a fourth-order R-K method along with shooting technique. The numerical values are obtained for the skin friction coefficient and local Nusselt number as well as the velocity and temperature profiles.

2. MATHEMATICAL FORMULATION

Consider a two-dimensional, steady, laminar, aligned magnetic flow of an electrically conducting and incompressible Casson fluid over a sheet coinciding with the plane $y < 0$, where the flow is confined to $y > 0$. Further, the extensible sheet occupies the negative x -axis and is moving continually in the positive x -direction with a velocity $u_s(x)$. The sheet somehow disappears in a sink that is located at $(x, y) = (0, 0)$. Furthermore, it is assumed that the surface of the sheet is heated to a variable temperature $T_W(x)$, which is higher than the ambient temperature T_∞ , the aligned magnetic field $B_0(x)$ is applied normal to the surface, with an acute angle α and it is fixed relative to the nanofluid, and induced magnetic field is assumed to be small, this implies a small magnetic Reynold number $(Re)_m = \mu_0\sigma U_0 x_0 \ll 1$, where μ_0 is the magnetic permeability, σ is the electrical conductivity of nanofluid, and U_0, x_0 are the characteristic velocity and reference length scales, respectively, and there is no applied voltage which implies the absence of an electrical field. We have considered two kinds of carbon nanotubes, namely SWCNTs and MWCNTs, to be used with water as the base fluid. The thermophysical properties of the nanofluids are given in Table 1.

The rheological equation for the incompressible flow of a Casson fluid is given by

$$\tau_{ij} = \begin{cases} 2 (\mu_B + p_y/\sqrt{2\pi}) e_{ij}, & \pi > \pi_c, \\ 2 (\mu_B + p_y/\sqrt{2\pi_c}) e_{ij}, & \pi < \pi_c. \end{cases}$$

Here $\pi = e_{ij}e_{ij}$ and e_{ij} are the (i, j) -th component of the deformation rate, μ_B is the plastic dynamic viscosity of the non-Newtonian fluid, p_y is the yield stress

Table 1. Thermophysical properties of base fluids and CNT's.

Physical properties	Base fluids	Nanoparticles	
	water	SWCNT	MWCNT
ρ [kg/m ³]	997	2600	1600
C_p [J/(kg · K)]	4179	425	796
k [W/(m · K)]	0.613	6600	3000

of the fluid, π is the product of the component of deformation rate with itself, and π_c is a critical value of this product based on the non-Newtonian model.

2.1. Flow analysis

The governing equations of the flow are given by

$$(2.1) \quad \frac{\partial u}{\partial x} + \frac{\partial v}{\partial y} = 0,$$

$$(2.2) \quad u \frac{\partial u}{\partial x} + v \frac{\partial u}{\partial y} = \nu_{nf} \left(1 + \frac{1}{\beta} \right) \frac{\partial^2 u}{\partial y^2} - \frac{\sigma B_0^2(x)}{\rho_{nf}} \sin^2 \alpha u,$$

with the boundary conditions

$$(2.3) \quad \begin{aligned} u &= u_s(x) + U_{slip}, & v &= 0 & \text{at} & y = 0, \\ u &= 0, & \text{as} & y \rightarrow \infty, & u &\rightarrow 0, & \text{as} & x \rightarrow -\infty, \end{aligned}$$

where (x, y) denotes the Cartesian coordinates along the sheet, u and v are the velocity components of the nanofluid along the x and y -axes, respectively, ν_{nf} is the kinematic viscosity of nanofluid, ρ_{nf} is the effective density of the nanofluid, β is the Casson fluid parameter ($\beta = \mu_B \sqrt{2\pi/p_y}$), and σ is the electrical conduction. These nanofluid quantities are defined as

$$(2.4) \quad \begin{aligned} \mu_{nf} &= \frac{\mu_f}{(1 - \phi)^{2.5}}, & \nu_{nf} &= \frac{\mu_{nf}}{\rho_{nf}}, & \rho_{nf} &= (1 - \phi) \rho_f + \phi \rho_{CNT}, \\ \alpha_{nf} &= \frac{k_{nf}}{(\rho C_p)_{nf}}, & \frac{k_{nf}}{k_f} &= \frac{(1 - \phi) + 2\phi \frac{k_{CNT}}{k_{CNT} - k_f} \ln \frac{k_{CNT} + k_f}{2k_f}}{(1 - \phi) + 2\phi \frac{k_f}{k_{CNT} - k_f} \ln \frac{k_{CNT} + k_f}{2k_f}}, \end{aligned}$$

where ϕ is the solid volume fraction, μ_{nf} is the effective dynamic viscosity, ρ_{nf} is the effective density, μ_f is the dynamic viscosity, ρ_f and ρ_s are the densities, k_{nf} is the thermal conductivity of nanofluid, k_f and k_{CNT} are the thermal conductivities of the base and carbon nanotubes respectively, $u_s(x)$ is considered in the form (KUIKEN [15]):

$$(2.5) \quad u_s(x) = \left(\frac{x_0}{|x|} \right)^n U_0, \quad n > 0.$$

U_{slip} is consider in the form (Wu [28]):

$$(2.6) \quad U_{slip} = \frac{2}{3} \left(\frac{3 - \alpha_m l^3}{\alpha_m} - \frac{3}{2} \frac{1 - l^2}{K_n} \right) \lambda_m \frac{\partial u}{\partial y} - \frac{1}{4} \left[l^4 + \frac{2}{K_n^2} (1 - l^2) \right] \lambda_m^2 \frac{\partial^2 u}{\partial y^2} = A \frac{\partial u}{\partial y} + C \frac{\partial^2 u}{\partial y^2}.$$

To convert the nonlinear partial differential equations into ordinary nonlinear differential equations, we introduce the self-similarity variables in the following form:

$$(2.7) \quad T_w(x) = T_\infty + T_0 \left(\frac{x_0}{|x|} \right)^m, \quad B(x) = B_0 \left(\frac{x_0}{|x|} \right)^{\frac{(n+1)}{2}},$$

$$\eta = y \left(\frac{u_s}{2v_f |x|} \right)^{1/2}, \quad f(\eta) = \frac{\psi}{(2v_f u_s |x|)^{1/2}},$$

$$\theta(\eta) = \frac{T - T_\infty}{T_w - T_\infty},$$

where T_0 is the characteristic temperature, B_0 is the uniform magnetic field, η is the similarity variable, $f(\eta)$ is the dimension less stream function, $\theta(\eta)$ is the dimensionless temperature, and ψ is the stream function which is defined by $u = \frac{\partial \psi}{\partial y}$ and $v = -\frac{\partial \psi}{\partial x}$. The above expression also satisfies the continuity Eq. (2.1). By using Eqs. (2.4)–(2.7), the Eq. (2.2) reduced to:

$$(2.8) \quad \frac{1}{(1 - \phi)^{2.5}} \left(1 + \frac{1}{\beta} \right) f''' + \left(1 - \phi + \phi \frac{\rho_{CNT}}{\rho_f} \right) [(n - 1) f f'' - 2n f'^2] - 2M \sin^2 \alpha f' = 0,$$

and the transformed boundary conditions are

$$(2.9) \quad f(0) = 0, \quad f'(0) = 1 + \lambda f''(0) + \delta f'''(0), \quad \text{at} \quad \eta \rightarrow 0,$$

$$f'(\eta) \rightarrow 0 \quad \text{as} \quad \eta \rightarrow \infty,$$

where $\lambda > 0$ and $\delta < 0$ are the first-order and second-order velocity slips, respectively, and $M = \sigma_f B_0^2 x_0 / \rho_f U_0$ is the magnetic parameter.

2.2. Heat transfer formulation

The boundary layer energy equation is given by

$$(2.10) \quad u \frac{\partial T}{\partial x} + v \frac{\partial T}{\partial y} = \frac{k_{nf}}{(\rho C_p)_{nf}} \frac{\partial^2 T}{\partial y^2} - \frac{1}{(\rho C_p)_{nf}} \frac{\partial q_r}{\partial y}.$$

Thermal radiation is simulated using the Rosseland diffusion approximation, and in accordance with this, the radiative heat flux q_r is given by

$$(2.11) \quad q_r = -\frac{4\sigma^*}{3k^*} \frac{\partial T^4}{\partial y},$$

where k^* is the Rosseland mean absorption coefficient and σ^* is the Stefan-Boltzmann constant. If the temperature differences within the mass of blood flow are sufficiently small, then Eq. (2.11) can be linearized by expanding T^4 into Taylor's series about T_∞ , and neglecting higher-order terms, we obtain

$$(2.12) \quad T^4 \cong 4T_\infty^3 T - 3T_\infty^4.$$

Therefore, Eq. (2.10) becomes

$$(2.13) \quad u \frac{\partial T}{\partial x} + v \frac{\partial T}{\partial y} = \frac{k_{nf}}{(\rho C_p)_{nf}} \frac{\partial^2 T}{\partial y^2} - \frac{16\sigma^* T_\infty^3}{3k^* (\rho C_p)_{nf}} \frac{\partial^2 T}{\partial y^2},$$

with the corresponding boundary conditions

$$(2.14) \quad \begin{aligned} T &= T_W(x), & \text{at} & \quad y = 0, \\ T &\rightarrow T_\infty & \text{as} & \quad y \rightarrow \infty, \quad x \rightarrow -\infty, \end{aligned}$$

where T_W is the wall temperature. By using self-similarity transformations of Eqs. (2.4)–(2.7), Eq. (2.13) is reduced to

$$(2.15) \quad \frac{1}{\text{Pr}} \left((1-\phi) + \phi \frac{(\rho C_p)_{\text{CNT}}}{(\rho C_p)_f} \right) \left(\frac{k_{nf}}{k_f} + \frac{4}{3} \text{Nr} \right) \theta'' + (n-1)f\theta' - 2m\theta f' = 0,$$

and the transformed boundary conditions are

$$(2.16) \quad \theta(0) = 1 \quad \text{at} \quad \eta \rightarrow 0, \quad \theta(\eta) \rightarrow 0 \quad \text{as} \quad \eta \rightarrow \infty,$$

where $\text{Pr} = \nu_f (\rho C_p)_f / k_f$ is the Prandtl number and $\text{Nr} = 4\sigma^* T_\infty^3 / k^* k_f$ is the radiation parameter. In this study, the quantities of practical interest are skin friction coefficient C_f and local Nusselt number Nu , which are defined as

$$(2.17) \quad C_f = \frac{\tau_w}{\rho_f u_s^2 / 2}, \quad \text{Nu} = \frac{x q_w}{k_f (T_w - T_\infty)},$$

where τ_w and q_w are the skin friction or the shear stress, and heat flux from the surface, respectively which are defined as

$$(2.18) \quad \tau_w = \mu_{nf} \left(\frac{\partial u}{\partial y} \right)_{y=0}, \quad q_w = -k_{nf} \left(\frac{\partial T}{\partial y} + q_r \right)_{y=0}.$$

Substituting Eq. (2.7) into (2.17) and (2.18), we obtain

$$\begin{aligned}
 \text{Re}_x^{1/2} C_f &= \sqrt{2} \frac{\mu_{nf}}{\mu_f} \left(1 + \frac{1}{\beta} \right) f''(0), \\
 \text{Re}_x^{-1/2} \text{Nu} &= -\frac{1}{\sqrt{2}} \left(\frac{k_{nf}}{k_f} + \frac{4}{3} \text{Nr} \right) \theta'(0),
 \end{aligned}
 \tag{2.19}$$

where $\text{Re}_x = \frac{u_s |x|}{\nu_f}$ is the local Reynolds number based on the stretching velocity $u_s(x)$.

3. NUMERICAL METHOD FOR SOLUTION

Equations (2.8) and (2.15) along with boundary conditions (2.9) and (2.16) form a two-point boundary value problem. These equations are solved using the fourth-order R-K method along with shooting technique, by converting them to an initial value problem. For this, we transform the non-linear ordinary differential Eqs. (2.8) and (2.15) to a system of first-order differential equations as follows:

$$\begin{aligned}
 f' &= z, & z' &= p, \\
 p' &= -\left(\frac{\beta(1-\phi)^{2.5}}{1+\beta} \right) \left\{ \left(1 - \phi + \phi \frac{\rho_{\text{CNT}}}{\rho_f} \right) [(n-1)fp - 2nz^2] - 2M \sin^2 \alpha z \right\}, \\
 \theta' &= q, & a &= \left((1-\phi) + \phi \frac{(\rho C_p)_{\text{CNT}}}{(\rho C_p)_f} \right), \\
 & & b &= \left(\frac{k_{nf}}{k_f} + \frac{4}{3} \text{Nr} \right),
 \end{aligned}
 \tag{3.1}$$

$$q' = -\frac{pr}{ab} ((n-1)fq - 2m\theta z).
 \tag{3.2}$$

The boundary conditions (2.9) and (2.16) becomes

$$\begin{aligned}
 f(0) &= 0, & f'(0) &= 1 + \lambda\omega_1 + \delta\omega_2, & \omega_1 &= f''(0), \\
 \omega_2 &= f'''(0), & \theta(0) &= 1.
 \end{aligned}
 \tag{3.3}$$

In order to integrate Eqs. (3.1) and (3.2) as initial value problem, we require values of $p(0)$, i.e., $f''(0)$, $q(0)$, i.e., $\theta'(0)$. However, no such values are given

at the boundary. So the suitable guess values for $f''(0)$ and $\theta'(0)$ are chosen, and the integration is carried out. The most important factor of this package is to choose an appropriate finite value of η_∞ . In order to determine η_∞ for the boundary value problem, start with some initial guess values for some particular set of physical parameters to obtain $f''(0)$ and $\theta'(0)$. The solving procedure is repeated with another value of η_∞ until two successive values of $f''(0)$ and $\theta'(0)$ differ only by the specified significant digit. The last value of η_∞ is finally chosen to be the most appropriate value of the η_∞ for that particular set of parameters. The value of η_∞ may change for another set of physical parameters. Once the finite value of η_∞ is determined, then the integration is carried out. Compare the calculated values for f' and θ at $\eta = 30$ (for example) with the boundary conditions $f''(30) = 0$ and $\theta'(30) = 0$ and adjust the estimated values $f''(0)$ and $\theta'(0)$, to give a better approximation to the solution. We take the series values for $f''(0)$ and $\theta'(0)$. The above procedure is repeated until the results up to desired degree of accuracy 10^{-6} are obtained.

4. RESULTS AND DISCUSSIONS

Figures 1–5 depict the dimensionless stream function $f(\eta)$, velocity profiles $f'(\eta)$, shear stress $f''(\eta)$ and temperature profiles $\theta(\eta)$ in SWCNT and MWCNT for various values of magnetic parameter M , nanoparticle volume fraction ϕ , first-order velocity slip parameter λ , aligned angle α , second-order velocity slip parameter δ . Figure 1 shows the dimensionless stream function $f(\eta)$, velocity profiles $f'(\eta)$, shear stress $f''(\eta)$ and temperature profiles $\theta(\eta)$ for various values of the magnetic parameter M for Newtonian and non-Newtonian fluids. The dimensionless stream function $f(\eta)$ and velocity profiles $f'(\eta)$ decrease and shear stress $f''(\eta)$ and temperature profiles $\theta(\eta)$ increase as the magnetic parameter M , increases for both Newtonian and non-Newtonian fluids. From these figures, we noticed that the behaviors at $M = 3.0$ for the non-Newtonian fluid and $M = 2.0$ for the Newtonian fluid are almost the same, and also the non-Newtonian fluids the same rapidly increase compare to the Newtonian fluids.

The effect of nanoparticle volume fraction ϕ on the dimensionless stream function $f(\eta)$, velocity profiles $f'(\eta)$, shear stress $f''(\eta)$ and temperature profiles $\theta(\eta)$ are shown in Fig. 2. Here, we notice that the dimensionless stream function $f(\eta)$, velocity profiles $f'(\eta)$ and temperature profiles $\theta(\eta)$ increase and the shear stress $f''(\eta)$ decreases as the nanoparticle volume fraction ϕ increases. From these figures, we observed that the behavior of $\phi = 0.3$ for the Newtonian fluid and $\phi = 0.2$ for the non-Newtonian fluid are slightly different, and also the Newtonian fluids rapidly increase compared to the non-Newtonian fluids for the profiles $f(\eta)$, $f'(\eta)$ and $f''(\eta)$ and the reverse trend is observed by the profile $\theta(\eta)$. Figure 3 displays the dimensionless stream function $f(\eta)$, velocity profiles $f'(\eta)$, shear

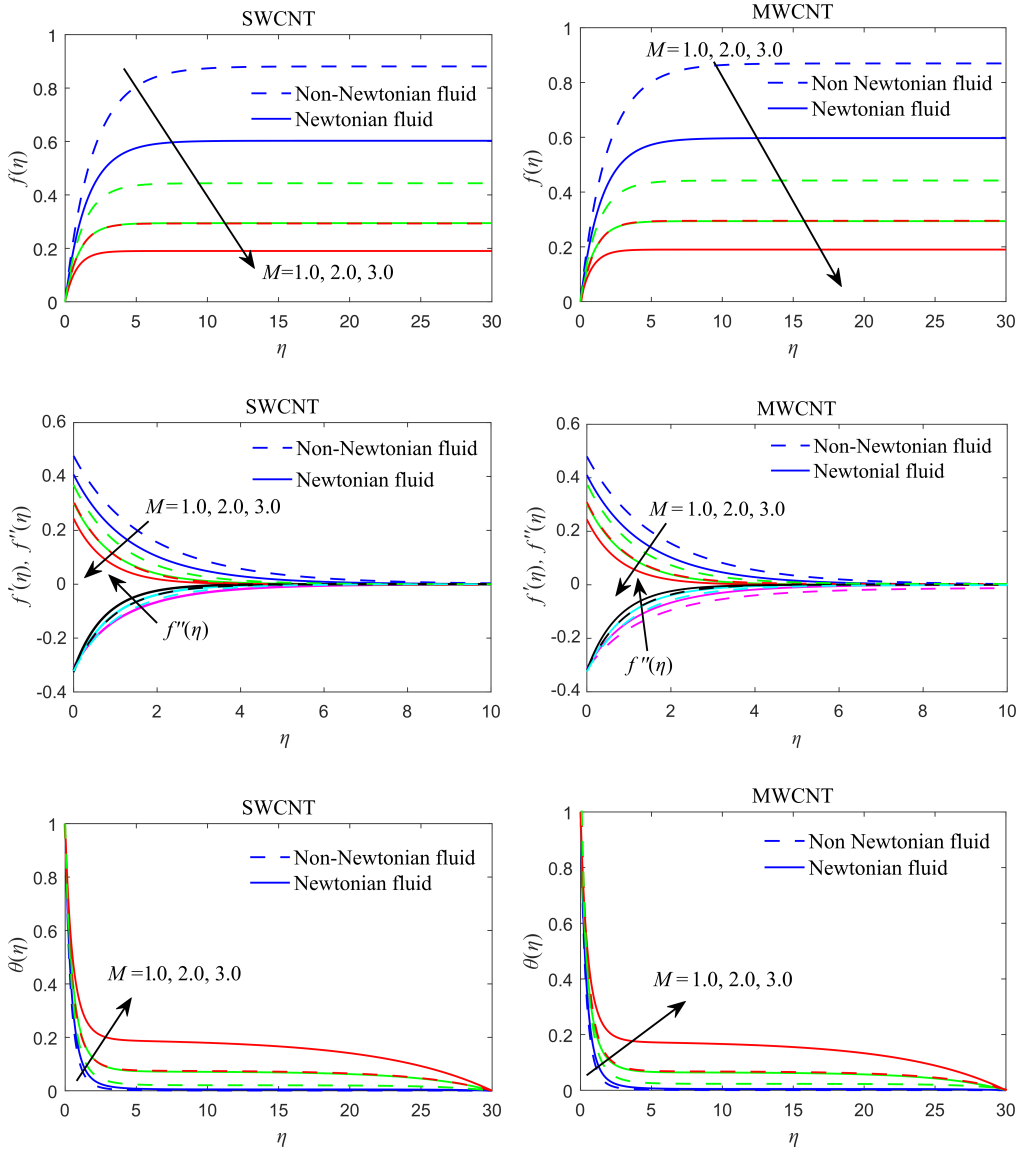


FIG. 1. The dimensionless stream function $f(\eta)$, velocity profiles $f'(\eta)$, and shear stress $f''(\eta)$, temperature $\theta(\eta)$ for different values of M .

stress $f''(\eta)$ and temperature profiles $\theta(\eta)$ for various values of aligned angle α . The dimensionless stream function $f(\eta)$ and velocity profiles $f'(\eta)$ decrease and shear stress $f''(\eta)$ and temperature profiles $\theta(\eta)$ increase as the aligned angle α increases. From these figures, we observed that the behavior of $\alpha = \pi/3$ for the non-Newtonian fluid and $\alpha = \pi/4$ for the Newtonian fluid are almost the same

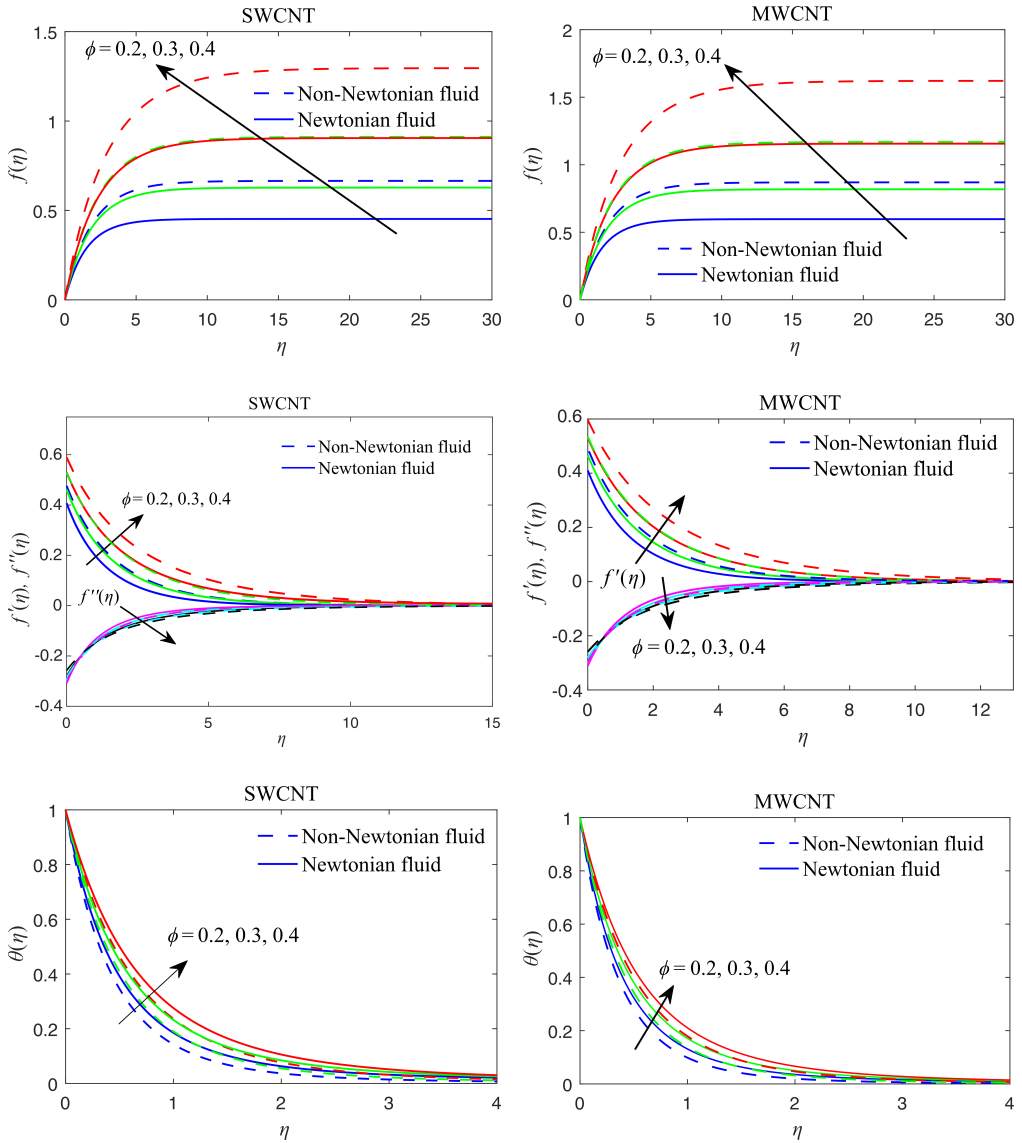


FIG. 2. The dimensionless stream function $f(\eta)$, velocity profiles $f'(\eta)$, and shear stress $f''(\eta)$, temperature $\theta(\eta)$ for different values of ϕ .

and also the non-Newtonian fluids rapidly increase compared to the Newtonian fluids.

The effect of second-order velocity slip parameter δ on the dimensionless stream function $f(\eta)$, velocity profiles $f'(\eta)$, shear stress $f''(\eta)$ and temperature profiles $\theta(\eta)$ are shown in Fig. 4 for both SWCNT and MWCNT. Here, we notice that the dimensionless stream function $f(\eta)$ and velocity profiles $f'(\eta)$ increase

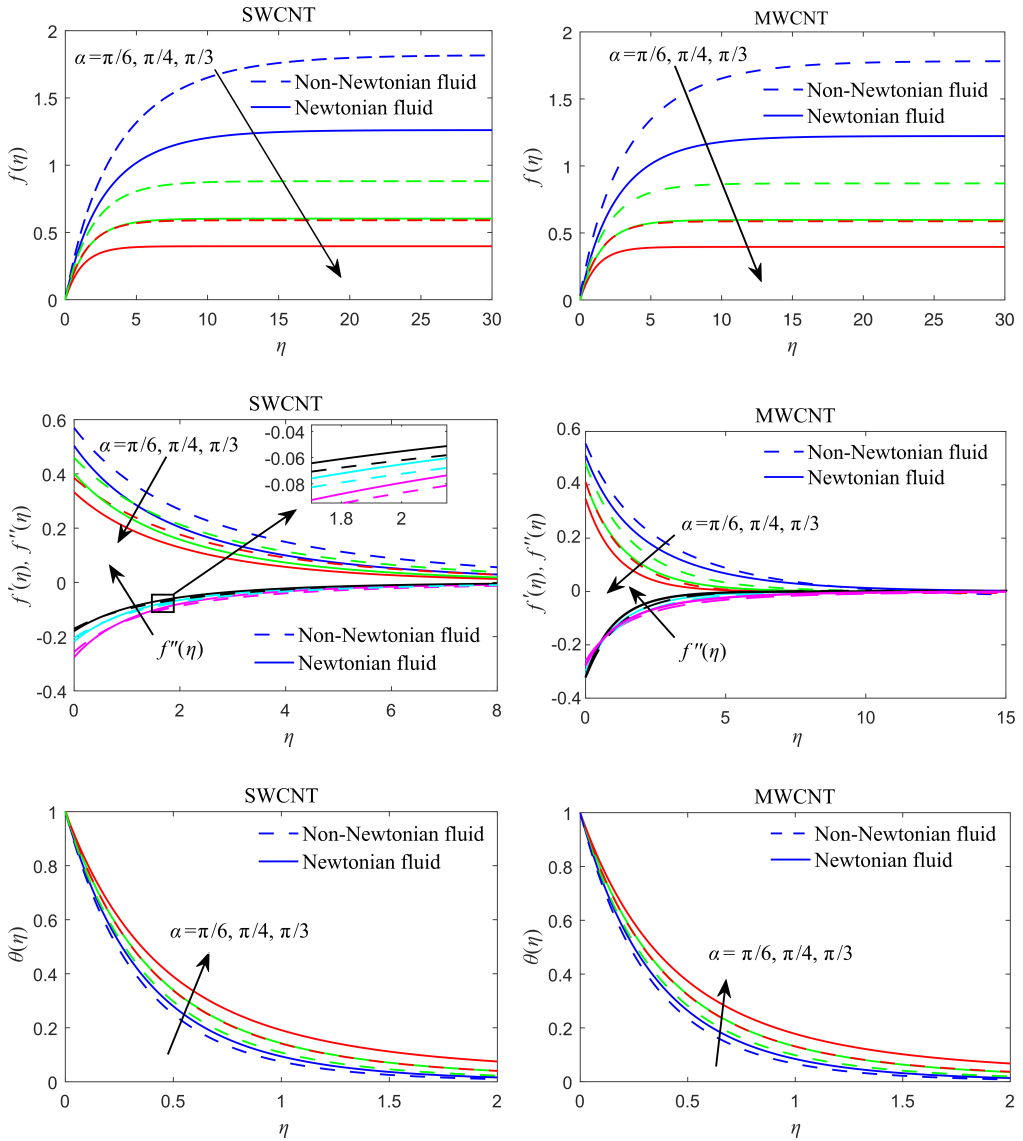


FIG. 3. The dimensionless stream function $f(\eta)$, velocity profiles $f'(\eta)$, and shear stress $f''(\eta)$, temperature $\theta(\eta)$ for different values of α .

and shear stress $f''(\eta)$ and temperature profiles $\theta(\eta)$ decrease as the second-order velocity slip parameter δ increases. From these figures, we observed that the non-Newtonian fluids rapidly increase compared to the Newtonian fluid for the profiles $f(\eta)$, $f'(\eta)$, $\theta(\eta)$, and $f''(\eta)$. Figure 5 displays the dimensionless stream function $f(\eta)$, velocity profiles $f'(\eta)$, shear stress $f''(\eta)$ and temperature

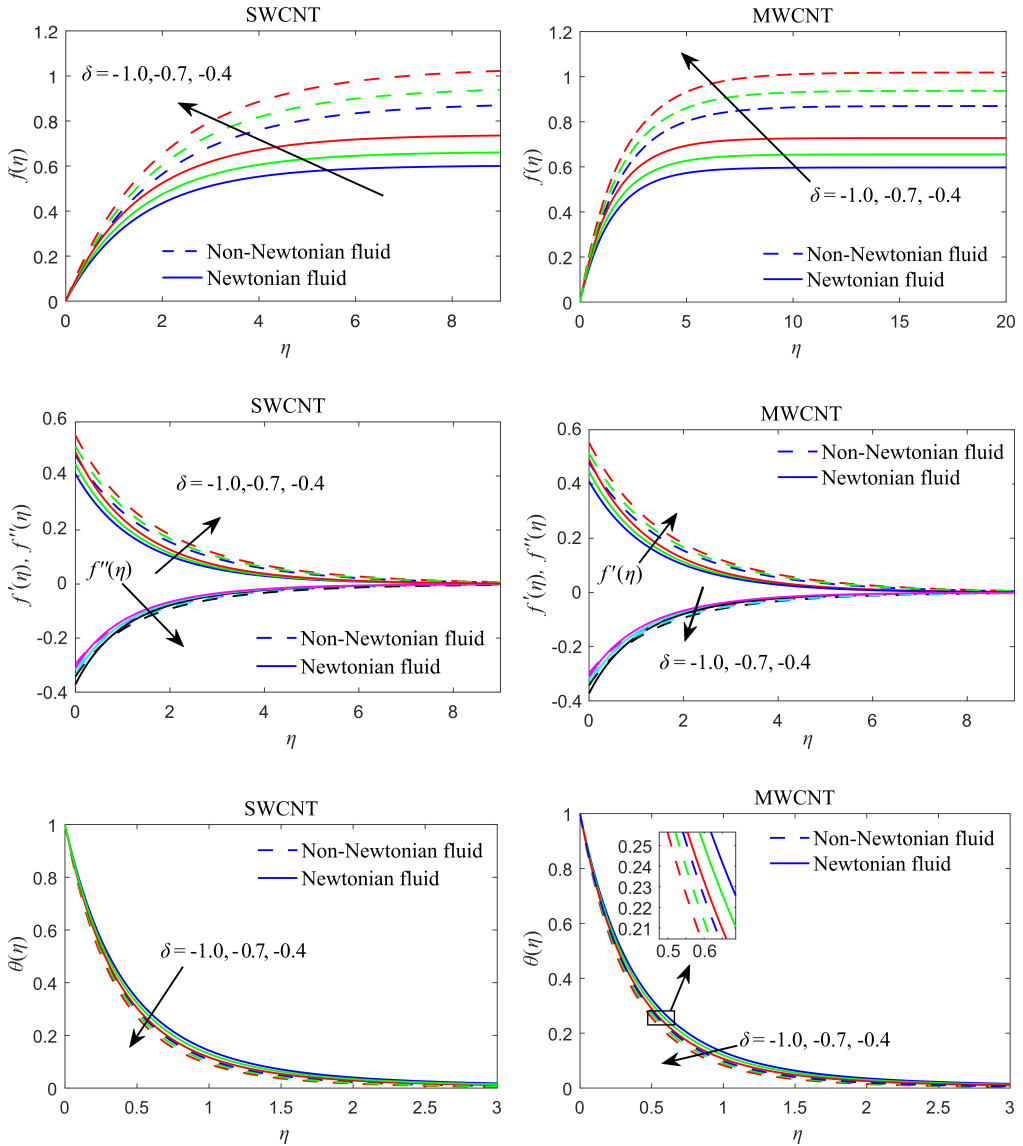


FIG. 4. The dimensionless stream function $f(\eta)$, velocity profiles $f'(\eta)$, and shear stress $f''(\eta)$, temperature $\theta(\eta)$ for different values of δ .

profiles $\theta(\eta)$ for various values of the first-order velocity slip parameter λ . The dimensionless stream function $f(\eta)$ and velocity profiles $f'(\eta)$ decrease and shear stress $f''(\eta)$ and temperature profiles $\theta(\eta)$ increase as the first-order velocity slip parameter λ increases. From these figures, we observed that the non-Newtonian fluids rapidly increases in comparison to the Newtonian fluids.

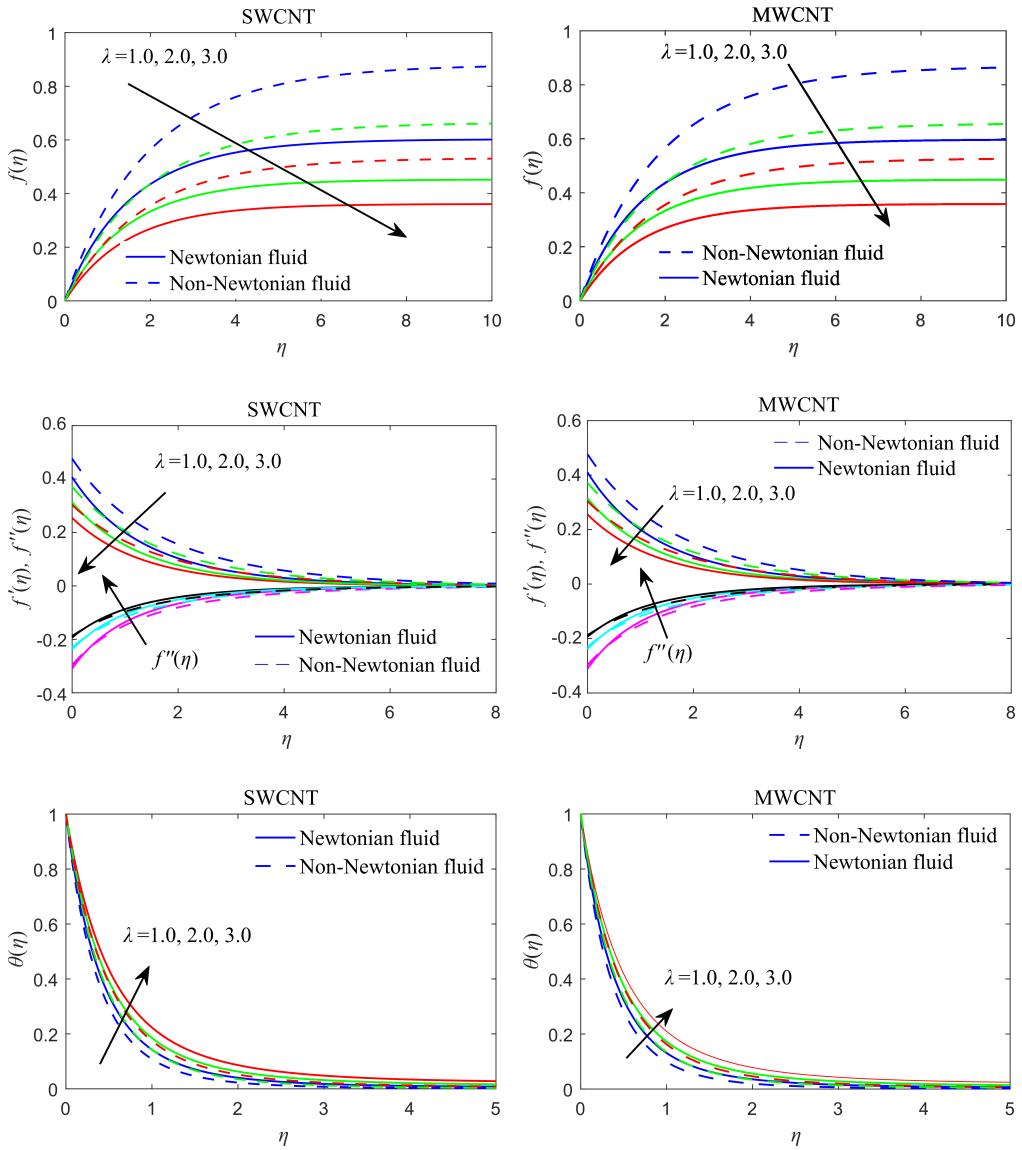


FIG. 5. The dimensionless stream function $f(\eta)$, velocity profiles $f'(\eta)$, and shear stress $f''(\eta)$, temperature $\theta(\eta)$ for different values of λ .

The thermophysical properties of base fluids and carbon nanotubes are shown in Table 1. Table 2 shows the validation of the present results with the with the results in published papers. We found the reasonable agreement. Table 3 displays the change in physical quantities at various parameters. It is noticed that the increasing values of magnetic parameter M , aligned angle α , velocity

Table 2. Validation of the present results for $f''(0)$ when $M = \phi = \lambda = \delta = 0$.

n	LIAO [14] $f''(0)$	KUDENATTI <i>et al.</i> [16] $f''(0)n^{-1/2}$	Present $f''(0)$
0.1	-0.215052		-0.21510
0.3	-0.519994		-0.52000
0.5	-0.744394		-0.74444
0.7	-0.926891		-0.92690
0.9	-1.083447		-1.08340
1.5		-1.19485	-1.19490
2.5		-1.22896	-1.22900
5.0		-1.25523	-1.25520
10.0		-1.26849	-1.26850
100.0		-1.28048	-1.28050

Table 3. Numerical values of skin friction coefficient $R_x^{1/2}C_f$ and local Nusselt number $R_x^{-1/2}Nu$.

M	ϕ	λ	δ	α	n	Nr	SWCNT		MWCNT	
							$R_x^{1/2}C_f$	$R_x^{-1/2}Nu$	$R_x^{1/2}C_f$	$R_x^{-1/2}Nu$
1.0	0.2	1.0	-1.0	$\pi/4$	0.2	0.7	-1.096690	11.716084	-1.102909	11.458016
1.5	0.2	1.0	-1.0	$\pi/4$	0.2	0.7	-1.163596	10.713106	-1.169159	10.475353
1.0	0.4	1.0	-1.0	$\pi/4$	0.2	0.7	-1.960473	17.380581	-1.972537	17.017411
1.0	0.2	1.5	-1.0	$\pi/4$	0.2	0.7	-0.959335	10.919137	-0.963641	10.671861
1.0	0.2	1.0	-0.8	$\pi/4$	0.2	0.7	-1.147390	11.996775	-1.152865	11.727257
1.0	0.2	1.0	-1.0	$\pi/2$	0.2	0.7	-1.194752	9.913679	-1.199450	9.696286
1.0	0.2	1.0	-1.0	$\pi/4$	0.4	0.7	-1.121608	11.285340	-1.124666	11.094323
1.0	0.2	1.0	-1.0	$\pi/4$	0.2	0.9	-1.096690	11.949379	-1.102909	11.702041

power index n , and radiation parameter Nr depreciate the skin friction coefficient and Nusselt number for both SWCNT and MWCNT. However, increasing the value of radiation parameter does not show a significant influence on the skin friction coefficient for both cases (SWCNT and MWCNT) and there is a slight increment on the Nusselt number for both cases. Increasing the values of second-order velocity slip parameter δ and nanoparticle volume fraction ϕ decreases the skin friction coefficient, and the reverse trend is observed for the Nusselt number.

5. CONCLUSION

The present paper analyzes the influences of the aligned magnetic field on the boundary layer flow of a Casson fluid over a stretching sheet in the presence

of carbon nanotubes with velocity slip effect. The governing partial differential equations are converted into ordinary ones by a similarity transformation, and then they are solved numerically by using the fourth-order R-K method along with shooting technique. The influence of the parameters M , ϕ , α , δ and λ on the dimensionless stream function $f(\eta)$, velocity profiles $f'(\eta)$, shear stress $f''(\eta)$ and temperature profiles $\theta(\eta)$ is presented. The numerical values are obtained for the skin friction coefficient and local Nusselt number as well as the velocity and temperature profiles:

- 1) $f(\eta)$ increases with increasing the nanoparticle volume fraction ϕ and second-order velocity slip parameter δ whereas the reverse trend is observed for the magnetic parameter M , first-order velocity slip parameter λ , and aligned angle α .
- 2) $f'(\eta)$ and $f(\eta)$ reduce for the non-Newtonian fluid compare to Newtonian fluid by increasing the M . $f''(\eta)$ and $\theta(\eta)$ increase for the Newtonian fluid in comparison to parameter the non-Newtonian fluid by increasing the M .
- 3) $f'(\eta)$ decreases with increasing the magnetic parameter M , first-order velocity slip parameter λ and aligned angle α . $f'(\eta)$ increases with increasing the nanoparticle volume fraction ϕ and second-order velocity slip parameter δ .
- 4) $\theta(\eta)$ increases with increasing the magnetic parameter M , nanoparticle volume fraction ϕ first-order velocity slip parameter λ , aligned angle α whereas the reverse trend is observed for the second-order velocity slip parameter δ .
- 5) The Nusselt number is greatly influenced by the nanoparticle volume fraction.
- 6) Increasing the value of the radiation parameter does not show a significant influence on the skin friction coefficient.

REFERENCES

1. REDDY P.B.A., REDDY B.N., *Thermal radiation effects on hydromagnetic flow due to an exponentially stretching sheet*, International Journal of Applied Mathematics and Computation, **3**(4): 300–306, 2012.
2. SRINIVAS S., REDDY P.B.A., PRASAD B.S.R.V., *Non-Darcian unsteady flow of a micropolar fluid over a porous stretching sheet with thermal radiation and chemical reaction*, Heat Transfer – Asian Research, **44**(2): 172–187, 2015.
3. HSIAO K.-L., *Stagnation electrical MHD nanofluid mixed convection with slip boundary on a stretching sheet*, Applied Thermal Engineering, **98**: 850–861, 2016.
4. AHMED J., BEGUM A., SHAHZAD A., ALI R., *MHD axisymmetric flow of power-law fluid over an unsteady stretching sheet with convective boundary conditions*, Results in Physics, **6**: 973–981, 2016.

5. BHATTI M.M., ABBAS T., RASHIDI M.M., *A new numerical simulation of MHD stagnation-point flow over a permeable stretching/shrinking sheet in porous media with heat transfer*, Iranian Journal of Science and Technology, Transactions A: Science, **41**(3): 779–785, 2017.
6. GUPTA S., KUMAR D., SINGH J., *MHD mixed convective stagnation point flow and heat transfer of an incompressible nanofluid over an inclined stretching sheet with chemical reaction and radiation*, International Journal of Heat and Mass Transfer, **118**: 378–387, 2018.
7. SAADATMANDI A., SANATKAR Z., *Collocation method based on rational Legendre functions for solving the magneto-hydrodynamic flow over a nonlinear stretching sheet*, Applied Mathematics and Computation, **323**: 193–203, 2018.
8. AFIFY A.A., *The influence of slip boundary condition on Casson nanofluid flow over a stretching sheet in the presence of viscous dissipation and chemical reaction*, Mathematical Problems in Engineering, **2017**: 1–12, 2017.
9. GHADIKOLAEI S.S., HOSSEINZADEH K., YASSARI M., SADEGHI H., GANJI D.D., *Boundary layer analysis of micropolar dusty fluid with TiO₂ nanoparticles in a porous medium under the effect of magnetic field and thermal radiation over a stretching sheet*, Journal of Molecular Liquids, **244**: 374–389, 2017.
10. SRINIVAS REDDY C., NAIKOTI K., RASHIDI M.M., *MHD flow and heat transfer characteristics of Williamson nanofluid over a stretching sheet with variable thickness and variable thermal conductivity*, Transactions of A. Razmadze Mathematical Institute, **171**(2): 195–211, 2017.
11. BHATTI M.M., RASHIDI M.M., *Effects of thermo-diffusion and thermal radiation on Williamson nanofluid over a porous shrinking/stretching sheet*, Journal of Molecular Liquids, **221**: 567–573, 2016.
12. KHAN M., SHAHID A., MALIK M.Y., SALAHUDDIN T., *Thermal and concentration diffusion in Jeffery nanofluid flow over an inclined stretching sheet: A generalized Fourier's and Fick's perspective*, Journal of Molecular Liquids, **251**: 7–14, 2018.
13. KHAN M., MALIK M.Y., SALAHUDDIN T., HUSSIAN A., *Heat and mass transfer of Williamson nanofluid flow yield by an inclined Lorentz force over a nonlinear stretching sheet*, Results in Physics, **8**: 862–868, 2018.
14. LIAO S., *On the homotopy analysis method for nonlinear problems*, Applied Mathematics and Computation, **147**(2): 499–513, 2004.
15. KUIKEN H.K., *On boundary layers in fluid mechanics that decay algebraically along stretches of wall that are not vanishingly small*, IMA Journal of Applied Mathematics, **27**(4): 387–405, 1981.
16. KUDENATTI R.B., AWATI V.B., BUJURKE N.M., *Approximate analytical solutions of a class of boundary layer equations over nonlinear stretching surface*, Applied Mathematics and Computation, **218**: 2952–2959, 2011.
17. MUKHOPADHYAY S., *Casson fluid flow and heat transfer over a nonlinearly stretching surface*, Chinese Physics B, **22**(7): 074701, 2013.
18. RAMESH K., DEVAKAR M., *Some analytical solutions for flows of Casson fluid with slip boundary conditions*, Ain Shams Engineering Journal, **6**(3): 967–975, 2015.

19. FARHAD ALI, NADEEM AHMAD SHEIKH, LLYAS KHAN, MUHAMMAD SAQIB, *Magnetic field effect on blood flow of Casson fluid in axisymmetric cylindrical tube: A fractional model*, Journal of Magnetism and Magnetic Materials, **423**: 327–336, 2017.
20. SUBBA RAO ANNASAGARAM, AMANULLA C.H., NAGENDRA N., SURYA NARAYANA REDDY M., BÉG O.A., *Hydromagnetic non-Newtonian nanofluid transport phenomena from an isothermal vertical cone with partial slip: Aerospace nanomaterial enrobing simulation*, Heat Transfer – Asian Research, **47**(1): 203–230, 2018.
21. PAL D., ROY N., *Lie group transformation on MHD double-diffusion convection of a Casson nanofluid over a vertical stretching/shrinking surface with thermal radiation and chemical reaction*, International Journal of Applied and Computational Mathematics, **4**(1): 1–23, 2018.
22. MUSTAFA M., KHAN J.A., *Model for flow of Casson nanofluid past a non-linearly stretching sheet considering magnetic field effects*, AIP Advances, **5**(7): 077148, 2015.
23. REDDY P.B.A., *Magnetohydrodynamic flow of a Casson fluid over an exponentially inclined permeable stretching surface with thermal radiation and chemical reaction*, Ain Shams Engineering Journal, **7**: 593–602, 2016.
24. REHMAN K.U., QAISER A, MALIK M.Y., ALI U., *Numerical communication for MHD thermally stratified dual convection flow of Casson fluid yields by stretching cylinder*, Chinese Journal of Physics, **55**: 1605–1614, 2017.
25. USMAN M., SOOMRO F.A., HAQ R.U., WANG W., DEFTERLI O., *Thermal and velocity slip effects on Casson nanofluid flow over an inclined permeable stretching cylinder via collocation method*, International Journal of Heat and Mass Transfer, **122**: 1255–1263, 2018.
26. REDDY P.B.A., *MHD boundary layer slip flow of a Casson fluid over an exponentially stretching surface in the presence of thermal radiation and chemical reaction*, Journal of Naval Architecture and Marine Engineering, **13**: 165–177, 2016.
27. REHMAN K.U., MALIK M.Y., ZAHRI M., TAHIR M., *Numerical analysis of MHD Casson Navier’s slip nanofluid flow yield by rigid rotating disk*, Results in Physics, **8**: 744–751, 2018.
28. WU L., *A slip model for rarefied gas flows at arbitrary Knudsen number*, Applied Physics Letters., **93**(25): 253103, 2008.

Received March 7, 2018; accepted version May 24, 2018.
